THE ANATOMICAL RECORD 303:1035–1042 (2020)

Estimating Flight Style of Early Eocene Stem Palaeognath Bird *Calciavis grandei* (Lithornithidae)

CHRISTOPHER R. TORRES [1]*, MARK A. NORELL [2,3] AND JULIA A. CLARKE [1,4]

[1]Department of Integrative Biology, University of Texas at Austin, Austin, Texas
[2]Richard Gilder Graduate School, American Museum of Natural History, New York, New York
[3]Division of Paleontology, American Museum of Natural History, New York, New York
[4]Jackson School of Geosciences, University of Texas at Austin, Austin, Texas

ABSTRACT

Lithornithids are volant stem palaeognaths from the Paleocene-Eocene. Except for these taxa and the extant neotropical tinamous, all other known extinct and extant palaeognaths are flightless. Investigation of properties of the lithornithid wing and its implications for inference of flight style informs understood locomotor diversity within Palaeognathae and may have implications for estimation of ancestral traits in the clade. Qualitative comparisons with their closest extant volant relatives, the burst-flying tinamous, previously revealed skeletal differences suggesting lithornithids were capable of sustained flight, but quantitative work on wing morphology have been lacking. Until comparatively recently, specimens of lithornithids preserving wing feather remains have been limited. Here, we reconstruct the wing of an exceptionally preserved specimen of the Early Eocene lithornithid *Calciavis grandei* and estimate body mass, wing surface area, and wing span. We then estimate flight parameters and compare our estimates with representatives from across Aves in a statistical framework. We predict that flight in *C. grandei* was likely marked by continuous flapping, and that lithornithids were capable of sustained flight and migratory behavior. Our results are consistent with previous hypotheses that the ancestor of extant Palaeognathae may also have been capable of sustained flight. Anat Rec, 303:1035–1042, 2020. © 2019 American Association for Anatomy

Key words: fossil; flying ability; wing loading; aspect ratio; Green River

Lithornithidae is an extinct clade of flying birds described from the earliest Paleogene to the Middle Eocene of Europe and North America (Houde, 1988; Parris and Hope, 2002). Lithornithids are closely related to Palaeognathae (ostriches, rheas, tinamous, emus, cassowaries and kiwi, as well as the recently extinct moa and elephant birds; Houde and Olson, 1981; Houde, 1988; Clarke, 2004; Nesbitt and Clarke, 2016), although their precise phylogenetic affinities are uncertain. Most recently, Nesbitt and Clarke (2016) recovered a lithornithid-tinamou clade next to the remaining palaeognaths in an unconstrained analysis of 182 morphological characters. However, lithornithids were recovered next to crown-group Palaeognathae (including tinamous) when relationships among extant palaeognaths were constrained to

Additional Supporting Information may be found in the online version of this article.

Grant sponsor: US National Science Foundation; Grant number: NSF EAR 1355292; Grant sponsor: University of Pennsylvania; Grant sponsor: Virginia Tech; Grant sponsor: University of Jinan.

*Correspondence to: Christopher R. Torres, Department of Integrative Biology, University of Texas at Austin, 2415 Speedway, C0930, Austin, TX 78712 E-mail: crtorres@utexas.edu

Received 8 July 2018; Revised 26 January 2019; Accepted 28 February 2019.

DOI: 10.1002/ar.24207
Published online 16 July 2019 in Wiley Online Library (wileyonlinelibrary.com).

match the topologies of recent molecular analyses (Phillips et al., 2010; Baker et al., 2014; Mitchell et al., 2014; Nesbitt and Clarke, 2016); we follow this placement in this article. Understanding the lithornithid wing morphology is thus important for elucidating flight characteristics within Palaeognathae as well for potentially shedding light on the early evolutionary history of the clade including the probability of dispersal and transitions to flight loss (Harshman et al., 2008; Mitchell et al., 2014; Yonezawa et al., 2017).

Efforts to characterize the lithornithid wing are rare. Those to date have relied on qualitative comparisons with extant birds (Houde and Olson, 1981; Houde, 1988). Although lithornithid body size is similar to extant tinamous, their closest volant relatives, key osteological differences in the sternum, forelimb, and pectoral girdle suggest functional differences in flight style (Houde and Olson, 1981; Houde, 1988; Nesbitt and Clarke, 2016). Flight in tinamous is typically reserved for escape and is characterized by short, powerful bursts (Davies, 2002). By contrast, Houde (1988) interpreted lithornithid skeletal anatomy as indicative of sustained flight, suggesting it "probably was characterized by slow, powerful wingbeats and intermittent periods of gliding" (Houde, 1988:135), similar to extant ibises and vultures. Quantitative evaluation of other key parameters related to flight (e.g., body mass [BM], wing shape and size) may improve such comparisons.

The fossil record cannot directly capture the behavioral or energetic aspects of flight, making flight characteristics difficult to estimate for extinct birds. Musculature typically does not fossilize and feathers are lost in all but the most exceptionally preserved specimens. However, in the presence of such exceptional preservation, the skeleton can be used to estimate simple parameters known to relate to flight characteristics like wing loading (a measure of the mass supported per unit of wing area) and aspect ratio (a measure of wing shape). Although these variables only provide simplified insights to flight capability, they are related to key characteristics of flight such as maximum flight velocity, take-off ability, maneuverability, and agility (Witter and Cuthill, 1993) and have been used to assess flight style in extant and extinct birds (Blem, 1975; Vickers-Rich and Scarlett, 1977; Campbell and Tonni, 1983; Burns and Ydenberg, 2002; Dial et al., 2006; Bowlin, 2007; Navarro et al., 2008; Ksepka, 2014), including investigations of flight loss (Livezey and Humphrey, 1986; Livezey, 1989).

Here, we investigate wing characteristics and estimate BM of an exceptionally preserved specimen of the Early Eocene lithornithid *Calciavis grandei* Nesbitt and Clarke (2016). Only two lithornithid specimens preserve wing feathering associated with the manus, and only one of these specimens preserves a nearly complete skeleton (Nesbitt and Clarke, 2016). We use this latter specimen to estimate BM, wing span, and wing surface area for *C. grandei* based on 20 alternative reconstructions with varying leading and trailing edge geometries. We then use these estimates to infer flight parameters for, and estimate the flight style of, *C. grandei.* Finally, we discuss implications for the evolution of flight within lithornithids and within Palaeognathae.

MATERIALS AND METHODS

Specimen

American Museum of Natural History (AMNH) 30560 is a specimen of *C. grandei* recovered from the Fossil Butte Member of the Early Eocene Green River Formation (51.66 ± 0.09 Ma) in Wyoming, preserving a nearly complete skeleton with associated feather remains (Nesbitt and Clarke, 2016). Dark, shadow-like carbonized feather traces surround most of the skeleton but lack detail everywhere except for the right wing, where the primary feathers are well-preserved (Fig. 1). The right wing is preserved in dorsal view with rachis and barb impressions clearly visible in primaries 2–9. The rachises of these feathers can be traced directly back to their points of insertion along the forelimb, including one on the proximal part of phalanx II-2, two on phalanx II-1, and five on the carpometacarpus; these last five also correspond to clear quill scars on the carpometacarpus, indicating that the primary feathers are preserved in life position relative to the manus. There are two additional quill scars on the carpometacarpus proximal to the previously mentioned five for which the corresponding primary

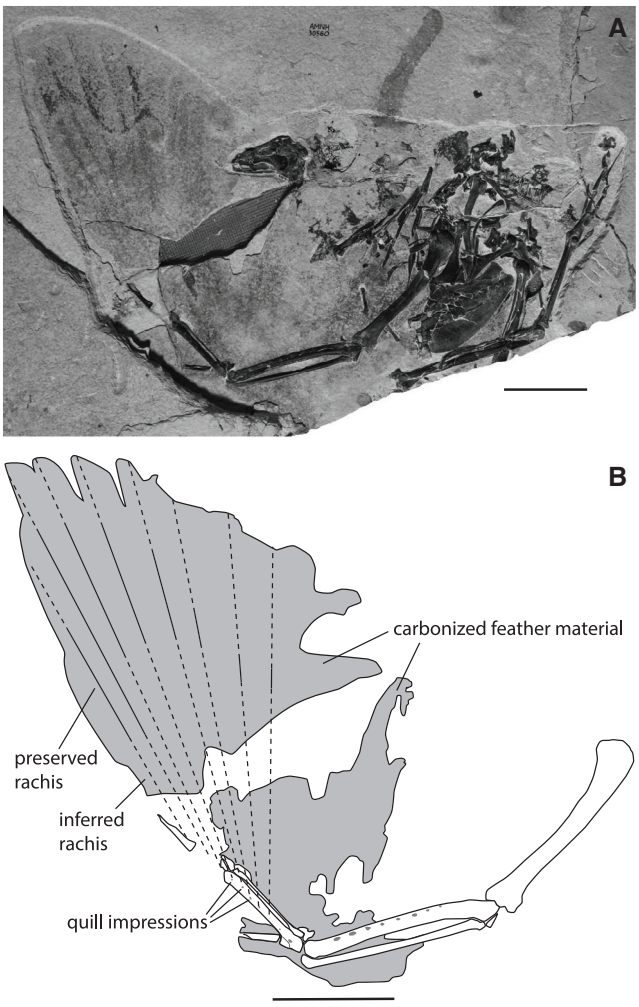

Fig. 1. (**A**) Slab specimen of Early Eocene lithornithid *Calciavis grandei* (AMNH 30560) with partially outstretched right wing. (**B**) Line drawing of AMNH 30560. Dark areas indicate regions of preserved feather material. The partial rachises of eight primary feathers are visible on the specimen, indicated by lines extending from the manus. Solid lines represent segments of preserved rachis, dashed lines represent reconstructed rachis projected proximally to the bone and distally to the ends of the feathers. Scale bars = 5 cm. Modified from Nesbitt and Clarke (2016).

feathers were not clearly preserved. Also, a final primary feather likely inserted on the distal part of phalanx II-2, as evidenced by what is likely a small, faintly preserved rachis impression; this feather was probably reduced, although this apparent reduction may be artifact of preservation. Thus, *C. grandei* likely had 11 primary feathers. Eleven primaries are also seen in waterfowl (Galloanseres), loons (Gaviidae), pelicans (Pelicanidae), herons (Ciconiidae), cormorants (Phalacrocoracidae), gulls and allies (Laridae), and cranes (Gruidae; Gadow, 1888; Lucas and Stettenheim, 1972; Van Tyne and Berger, 1976). By contrast, 10 are observed in tinamous, 12 in kiwi, emus and rheas, and extremes are observed in ostriches (18) and cassowaries (2; Gadow, 1888). The tips of the distal-most primary feathers are well preserved and characteristically asymmetrical. By contrast, the secondary feathers are poorly preserved, represented by amorphous carbonized traces across only part of the area they would have occupied in life, exhibiting little detail beyond some barb impressions. The distal extent of the secondary and tertiary feathers is not preserved.

Wing Reconstruction and Wing Area

The wing of AMNH 30560 is only partially outstretched and likely does not reflect a life-like flight position. The avian wing achieves a wide range of positions throughout the flight stroke; to simplify comparisons, we estimated the fully outstretched *C. grandei* wing as a proxy for overall flying position. To estimate this position, the angle between the leading edges of the carpometacarpus and radius were averaged for four *Nothura maculosa* and three *Nothura darwinii* spread wing mounts (Table S1) and used to predict the corresponding angle in AMNH 30560. These species are both extant tinamous and were chosen based on availability of spread wing comparative material. Both these species fly in short, rapid bursts in response to danger and occupy high-altitude grassland, possibly biasing our reconstruction toward a wing shape adapted to such habitat. However, we assume that the variation in overall wing shape across birds with different flight styles caused by differences in angles between elements of the forelimbs was insignificant compared to variation caused by differences in flight feather size, shape, and number. The manus and corresponding primary feather material of AMNH 30560 were digitally rotated with respect to the wrist joint in Adobe Illustrator CC 2017 to reflect the reconstructed angle. The humerus was rotated with respect to the elbow joint until the proximal end encountered the line defined by the leading edge of the carpometacarpus (Fig. 2).

We reconstructed the wing of AMNH 30560 with five different shapes (Fig. 2A–E). In each case, the outline of the wing was reconstructed as segments based on how they were reconstructed. In all cases, the segments representing the leading edge of the wing and the tip of the wing (Fig. 2A–E, segments i–ii and ii–iii) were reconstructed identically. The leading edge (including the membrane extending from the shoulder to the wrist, i.e., the propatagium) was defined by the leading edge of the carpometacarpus and extended from the proximal end of the humerus to the distal end of manual digit II:2. Because the propatagium was not preserved, it is unknown how much it contributed to overall wing surface area; to account for this uncertainty, versions of all reconstructions were made that both included and excluded the area defined by the cranial margins of the radius and humerus and the leading edge of the wing (Fig. 2). The tip of the wing was reconstructed by directly tracing the preserved primary feathers.

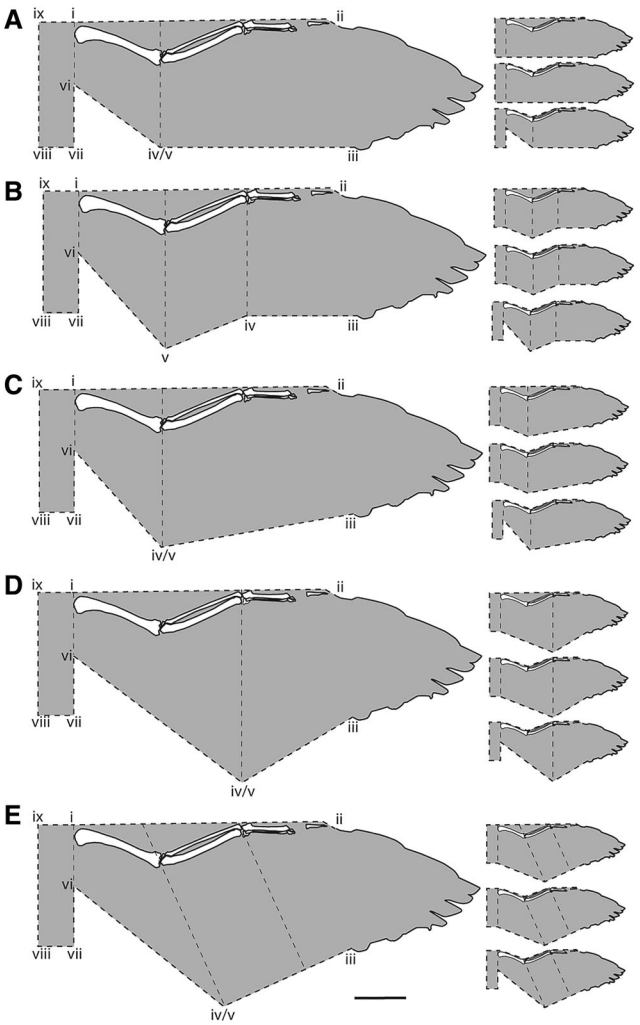

Fig. 2. Reconstructions of the fully outstretched wing of *Calciavis grandei* (AMNH 30560). (**A**–**E**) Alternative reconstructions of the shape of the trailing edge. The border of the wing is divided into segments based on how the border was reconstructed. The border of the tip of the wing was based directly on the preserved border of the primaries, indicated by a solid line. The rest of the border was reconstructed, indicated by a dashed line. See the text for explanation of the methods for border reconstruction. Primary reconstructions including propatagium and short tertiary feathers. Reconstruction permutations: 1, main reconstructions with short tertiary feathers and with propatagium; 2, long tertiary feathers with propatagium; 3, long tertiary feathers with no propatagium; and 4, short tertiary feathers with no propatagium. Scale bar = 5 cm.

The wing reconstructions differ by how the trailing and proximal edges of the wing (i.e., the secondary and tertiary feathers) were estimated. Reconstruction A (Fig. 2A) is the simplest and likely the least realistic, with a perfectly straight trailing edge (segment iii–iv/v) parallel to the leading edge and extending proximally from the point where the primary feathers are no longer preserved to the proximal edge of the wing. In reconstruction B (Fig. 2B), line segment iii–iv is parallel to the manus and extends from the preserved primary feathers to the

proximal end of the carpometacarpus; the length and angle of line segments iv–v and v–vi are defined by the cranial margins of the radius and humerus, respectively.

Reconstructions C and D (Fig. 2C,D) are similar to reconstruction B except that line segment iv–v has been collapsed into a single point iv/v. C and D differ from each other by the position of point iv/v; in C, it is defined by the distal end of the humerus; in D, it is defined by the distal end of the radius. In both cases, the angle of line segment iii–iv/v depends on the position of point iv/v. In reconstruction E (Fig. 2E), like C and D, line segment iv–v is collapsed into a single point iv/v; like B, the trailing edge of E comprises lines (segments iii–iv/v and iv/v–vi) parallel to the cranial margins of the radius and humerus, respectively. The position of point iv/v in reconstruction E is determined by a line perpendicular to segment iii–iv/v and intersecting the point of articulation of the ulna and humerus.

Typically, surface area is measured from both wings as well as the inter-wing area (Pennycuick, 1989). Unfortunately, the body of AMNH 30560 is not preserved in three dimensions and so direct measurement of the inter-wing area is impossible. However, Nudds and Rayner (2006) observed that avian body width typically accounts for $4.12 \pm 0.11\%$ of total wing span. This observation was used to estimate mean, minimum and maximum inter-wing span for AMNH 30560. These values were used to estimate mean, minimum and maximum wing area, respectively, for each wing reconstruction. The inter-wing span reconstructed for AMNH 30560 is depicted in all reconstructions (Fig. 2) by line rectangle i/vii/viii/ix.

We considered the five reconstructions with propatagia and short tertiaries to be our main reconstructions (Fig. 2A1–E1). However, all statistical analyses were also carried out using the complete set of alternative reconstructions (Table S3). Each primary reconstruction was modified to either lack a propatagium (Fig. 2A4–E4), have elongate tertiaries (Fig. 2A2–E2), or both (Fig. 2A3–E3). In the main reconstructions, the propatagium was reconstructed as a straight line from the wrist joint to the shoulder; the area defined by this line and the anterior margins of the radius and humerus was excluded to estimate wing area without the propatagium. In all reconstructions with short tertiaries, the point where the trailing edge of the wing intersects with the body (point iv) is defined as the midpoint of line segment i-vii. To reflect long tertiary feathers, the point where the wing encounters the reconstructed inter-wing area was moved to point vii.

Body Mass Estimation

Field et al. (2013) identified and assessed skeletal correlates for BM in neognath birds, including length, diameter, and circumference of the humerus, femur, and tarsometatarsus, as well tibiotarsus length, coracoid shaft width and length, and length of the coracoid component of the glenoid facet. Because AMNH 30560 is preserved in a slab and is missing most of both femora, only humerus, tarsometatarsus, and tibiotarsus length can be directly measured. Of these correlates, length of the humerus had the most predictive power (Field et al., 2013) and was used in all statistical analyses. The equation for relating BM to humeral length (HL) used herein is provided in Supporting Information. The equations derived by Field et al. (2013) used data that did not include palaeognaths; however, the humeri of the volant lithornithids are likely under ecological constraints more like the flying neognaths than the nonflying ratites so a neognath-like relationship between HL and BM can be reasonably expected for AMNH 30560.

Total Reconstruction Sample

To account for ranges of error in our estimations, we conducted all downstream statistical analyses using every combination of minimum, mean and maximum estimate of BM, wing span and wing area for all 20 alternative wing shape reconstructions, resulting in a total of 540 combinations for *C. grandei.* Our discussion focuses on the analyses using the mean values for our five main wing shape reconstructions, referred henceforth our main reconstructions (Fig. 2A1–E1).

Flight Modeling

To compare flight parameters across our sample, we estimated power curves for all 540 *C. grandei* reconstructions as well as 152 extant flying neognaths using data from Bruderer et al. (2010). Power curves model aerodynamic power required to maintain flapping flight over a range of true airspeeds, the minimum and maximum bounds of which are defined by the minimum power speed (*V*mp) and the maximum range speed (*V*mr), respectively. *V*mp is the speed at which mechanical power required to maintain flapping flight is minimized (Thomas and Hedenstrom, 1998). *V*mr is the greatest speed requiring the least power; that is, the speed at which fuel consumption per unit distance is minimized (Pennycuick, 1975; Thomas and Hedenstrom, 1998).

For each species or *C. grandei* reconstruction, we used BM, wing span, and wing area to estimate *V*mp and *V*mr in R (R Core Team, 2018) using the findMinimumPowerSpeed() and findMaximumRangeSpeed() functions, respectively, in the afpt R package (KleinHeerenbrink, 2017). We rounded those values down (for *V*mp) or up (for *V*mr) to the nearest 0.1 m/s, and then estimated mechanical power required to maintain flapping flight within that range at intervals of 0.1 m/s using the equations of Pennycuick (1989). In all cases, we assumed air density at sea level (1.23 kg/l^3) and standard acceleration due to gravity (9.81 m/s^2). Although this assumption may disregard differences in environmental conditions experienced by these birds in life, it provides a useful baseline for comparison. We also estimated the reference wingbeat frequency used in cruising flight in each case using the equation of Pennycuick (1989). We then derived and graphed polynomial formulae describing each power curve in R. For detailed methods including equations and parameter values used, see Supporting Information.

Statistical Analysis and Comparison with Other Birds

We used linear discriminate analysis (LDA) of the Bruderer et al. (2010) dataset to predict the flight style of *C. grandei.* Bruderer et al. (2010) categorized each species in their dataset as one of four broad flight styles, elaborating on categories proposed by Pennycuick (2008): continuous flapping (CF), soaring (S), flapping-gliding (FG), and flapping-bounding (i.e., passerine-type; FB). LDA was used to characterize each flight style based on BM, wing

span, and wing surface area in R (R Core Team, 2018) using the lda() function in the MASS package (Venables et al., 2002). These results were then used to predict flight style in all 540 alternative *C. grandei* reconstructions based on the same variables using the predict() function in the MASS package. All values for all statistical analyses were log transformed. To allow direct comparison of physical parameters, we also regressed aspect ratio on BM. Data used in statistical analyses are provided in Tables S2 and S3.

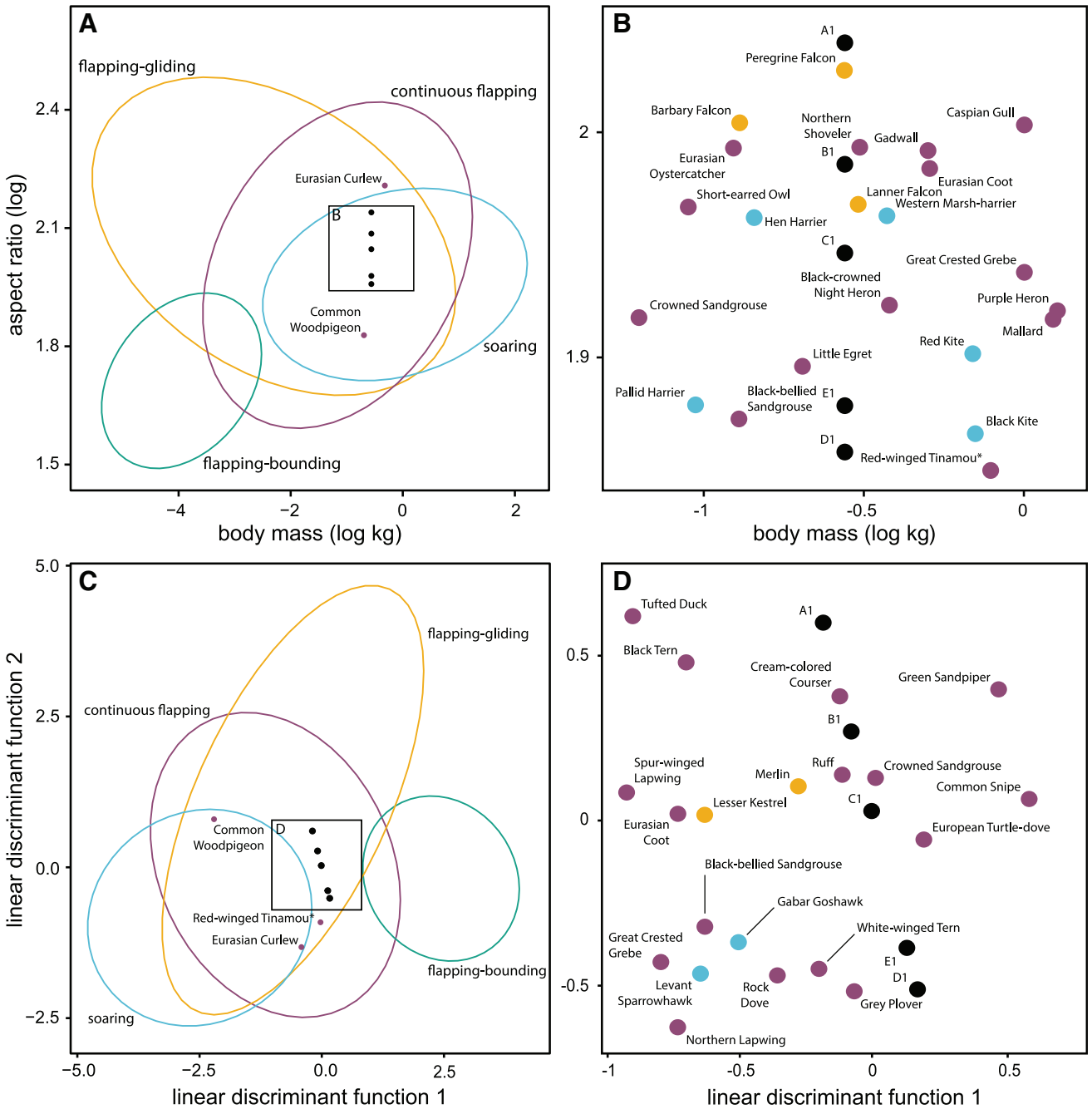

Fig. 3. Comparison of our five main reconstructions of mean body mass, wing surface area, and wing span for the flying stem palaeognath *Calciavis grandei* with 152 flying extant birds. (**A**) Aspect ratio versus body mass; (**B**) zoom in on highlighted region in A; (**C**) the first two discriminant functions of our linear discriminant analysis, explaining 81% (primarily influenced by wing area) and 18% (primarily influenced by wing span) of variation, respectively; (**D**) zoom in on highlighted region in C. Common Woodpigeon and Eurasian Curlew are indicated in A and C because they exhibit similar power curves to our main lithornithid reconstructions (Fig. 4). Asterisks indicate birds that do not show at least partial migratory behavior. Ellipses represent 95% confidence intervals for flight styles. Detailed figures and graphs of linear discriminant function 3, and including all 540 lithornithid reconstructions, are provided in Figures S1-2. Colors: black, main *C. grandei* reconstructions (Fig. 2); purple, continuous flappers; yellow, flapping-gliders; blue, soaring birds; and green, flap-bounders.

RESULTS

Estimates of Physical Parameters for *C. grandei*

An average angle of 159.26-degrees was observed between the leading edges of the carpometacarpus and radius in seven tinamou spread wing mounts (Table S1). The wing of AMNH 30560 was preserved at an angle of 123.7-degrees, leading to suggested adjustment of 35.56-degrees. The estimated inter-wing span for AMNH 30560 was 0.034 ± 0.0009 m, resulting in a total wingspan of 0.82 ± 0.0009 m. Average estimated wing area for our main reconstructions (including propatagium and short tertiary feathers) were 0.078–0.089 m^2. BM for the AMNH 30560 specimen of *C. grandei* estimated from humerus length was 570.69 g, with a 95% prediction interval (PI) of 0.23–1.39 kg. All estimates are provided in Table S3.

Statistical Analyses

When aspect ratio is graphed against BM, all five main *C. grandei* reconstructions (Fig. 3A,B) and nearly all 540 reconstructions fall within the 95% confidence ellipses of CF, FG, and soaring birds, with none overlapping with FB.

Our LDA of BM, wing surface area, and wing span yielded three discriminant functions, explaining 0.88, 0.09, and 0.03 of the variance in our data, respectively (Fig. 3, Fig. S1). Our analysis predicted a (CF) flight style for *C. grandei* for all possible combinations of minimum, mean, and maximum values for each physical parameter, but posterior probably (PP) was particularly sensitive to BM. All analyses using mean or maximum BM supported CF with PP > 0.9; analyses using minimum BM only supported it with PP = 0.57–0.67, followed by flap gliding (PP = 0.09–0.36) and soaring (PP = 0.07–0.25). Results of our LDA (group means and linear discriminant coefficients) as well posterior probabilities from all classifications are provided in Table S4. Linear discriminant functions 1 and 2 including only our main *C. grandei* reconstructions are graphed in Figure 3C,D. All three functions with all 540 reconstructions are graphed in Figure S2.

Estimates of Flight Parameters

The power curves for our five main *C. grandei* reconstructions share parameter space with soaring and (CF) birds are just above the upper range of flap-gliding birds and are well above flap-bounding birds (Fig. 4A). The power curves for Eurasian Curlew and especially the Common Woodpigeon are the most like *C. grandei* (Fig. 4B). When all 540 alternative reconstructions are considered, *C. grandei* occupies a wide portion of parameter space and power curves are clustered based on whether minimum, mean, or maximum BM was used in the analysis (Fig. S3).

DISCUSSION

Our quantitative comparisons of the Early Eocene lithornithid *C. grandei* to extant birds based on reconstructions of BM and wing shape suggest that these stem palaeognaths were likely continuous flappers capable of sustained flight and may have been migratory. We predict ranges of aerodynamic power required for flight and optimal airspeed for *C. grandei* that are most like the *CF* Common Woodpigeon and Eurasian Curlew among our comparative sample (Fig. 4); thus, these species are likely the best analogues for flight in *C. grandei*. *CF* birds are

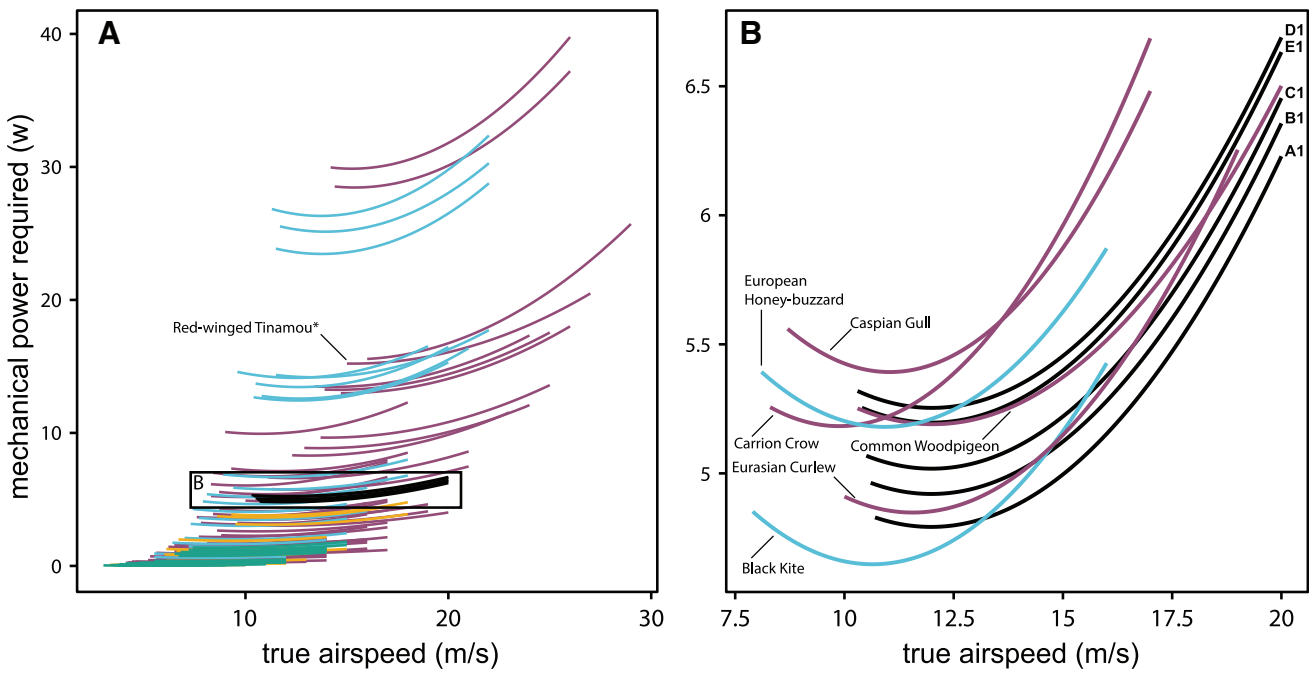

Fig. 4. Mechanical power required to maintain flapping flight versus true airspeed of our five main *C. grandei* wing reconstructions compared with: (**A**) all 152 extant flying birds in our comparative sample; and (**B**) only those birds with power curves most like our reconstructions. Asterisks indicate birds that do not show at least partial migratory behavior. A more detailed graph including power curves estimated for all 540 lithornithid reconstructions is provided in Figure S3. Colors: black, main *C. grandei* reconstructions (Fig. 2); purple, continuous flappers; yellow, flapping-gliders; blue, soaring birds; and green, flap-bounders.

represented in our dataset by tinamous, water- and landfowl, shorebirds, corvids (e.g., ravens, crows), flamingos, grebes, and owls, all of which exhibit a wide range of behaviors and ecologies. Indeed, the Common Woodpigeon and Eurasian Curlew occupy vastly different niches, and exhibit widely disparate wing aspect ratios despite similar wing loadings (Table 1, Fig. 3C). However, both these species are capable sustained flyers and are mostly migratory, suggesting *C. grandei* may have been capable of similar behavior.

Our results also suggest that lithornithids were more capable long-distance flyers than their most closely related extant volant taxon, the tinamous. Tinamous, which were represented in our dataset by the Red-winged Tinamou, are continuous flappers and reserve flight for rapid, evasive bursts to escape danger. Accordingly, the Red-winged Tinamou has a wing loading approximately double our main reconstructions of *C. grandei.* Increases in wing loading generally correspond to decreases in flying maneuverability and increases in both power required to take off and maintain flight, as well as increases in required airspeeds. Correspondingly, the Red-winged Tinamou requires approximately triple the aerodynamic power to maintain flapping flight required by *C. grandei* at similar airspeeds (Fig. 4A). An important caveat to this comparison is that birds relying on burst flight, like tinamous, may be adapted to optimize flight performance at near-zero airspeed, and so the power curve estimated here may not reflect true optimal flight speeds (Thomas and Hedenstrom, 1998).

TABLE 1. Estimated wing loading (WL), aspect ratio (R_a), reference wingbeat frequency (f_{ref}), and fight style (FS) for our primary wing reconstructions of Early Eocene lithornithid *Calciavis grandei* compared with representatives across Aves

Species	FS	R_a	WL	f_{ref}
Black Tern	CF	6.9	1.2	4.5
Gabar Goshawk	S	6.5	2.3	5.3
Pallid Harrier	S	7.2	2.3	3.5
Lesser Kestrel	FG	6.9	2.4	5.4
Short-eared Owl	CF	7.9	2.6	3.7
Cream-colored Courser	CF	7.2	2.8	6.8
Hen Harrier	S	7.9	2.8	3.6
Red Kite	S	7.4	2.8	2.8
Western Marsh-Harrier	S	7.9	2.9	3.1
Green Sandpiper	CF	7	3	8.1
Levant Sparrowhawk	S	6.6	3	5.5
Black Kite	S	7.1	3.1	3.1
European Honey-buzzard	S	6.2	3.1	3.3
Merlin	FG	7.1	3.2	6.6
European Turtle-dove	CF	6.8	3.3	7.4
Carrion Crow	CF	5.9	3.8	4.7
Gray Plover	CF	6.5	3.8	6.9
Common Snipe	CF	6.8	3.9	8.8
Caspian Gull	CF	8.2	4	3.3
Black-crowned Night Heron	CF	7.6	4.1	4.2
Lanner Falcon	FG	7.9	4.2	4.3
Ruff	CF	7.2	4.2	7.5
Little Egret	CF	7.4	4.3	5
Eurasian Oystercatcher	CF	8.1	4.5	5.4
Peregrine Falcon	FG	8.4	5.2	5.1
Rock Dove	CF	6.9	5.4	7.1
Common Woodpigeon	CF	6.2	5.5	6.6
Barbary Falcon	FG	8.2	5.7	6.4
Black-bellied Sandgrouse	CF	7.2	5.7	6.8
Calciavis grandei† (D1)	CF*	7.1	6	6.2
Calciavis grandei† (E1)	CF*	7.2	6.1	6.3
Eurasian Curlew	CF	9.1	6.1	5
Calciavis grandei† (C1)	CF*	7.7	6.5	6.4
Calciavis grandei† (B1)	CF*	8.1	6.8	6.5
Crowned Sandgrouse	CF	7.5	6.9	9
Calciavis grandei† (A1)	CF*	8.5	7.2	6.6
Gadwall	CF	8.1	7.4	6.2
Northern Shoveler	CF	8.1	8	7.2
Eurrasian Coot	CF	8	10.6	8.3
Great Crested Grebe	CF	7.7	11.7	8.1

Flight styles: FB, flapping-bounding; CF, continuous flapping (*predicted); FG, flapping-gliding; S, soaring. Data for Red-winged Tinamou from Alerstam et al. (2007) and for the rest from Bruderer et al. (2010). Full comparative dataset provided in Table S2. All ranges of estimated values for lithornithids provided in Table S3.
†Extinct taxa.

The proportional size and shape of the wings of *C. grandei* further suggest lithornithids were better suited to sustained flight than tinamous. All 20 of our alternative wing reconstructions for *C. grandei* had markedly pointed primary feathers (Fig. 2), consistent with the shape of the wingtip preserved in an isolated lithornithid wing (FMNH [Field Museum of Natural History] PA 729, gen. and sp. indet) described by Nesbitt and Clarke (2016). Correspondingly, our main *C. grandei* wing reconstructions had higher aspect ratios than the Red-winged Tinamou (Table 1, Fig. 3B), consistent with the observations of Houde (1988). Aspect ratio has implications for flight performance: increases in aspect ratio correspond to increases in the generation of lift and decreases in drag; thus, the proportionally longer wings of *C. grandei* were better adapted to sustained flight than the Red-winged Tinamou. A complicating factor to comparisons of aspect ratio, however, is their inability to account for wing tip slotting, a behavior which can also increase lift production (Savile, 1957).

Ranges of error in our estimates of *C. grandei* BM impacted our analyses more strongly than ranges of error in wing span or surface area (Figs. S1–3). Further reducing uncertainty in BM estimates in extinct taxa is key to improving such analyses. Our estimate of BM for AMNH 30560 yielded a 95% PI spanning an order of magnitude (234.36–1,389.71 g). This interval encompasses the entire range of average BMs for extant tinamous (Dunning, 2008) and so both extremes are biologically feasible, but improved estimates of BM with narrower ranges of error will better constrain biological interpretation. It must also be noted that the equation used to estimate BM was based on the most extensive survey to date but also one that excluded palaeognath birds, including tinamous (Field et al., 2013). Our exploration of sources of error highlights other variables that must also be accounted for when estimating flight parameters and style for extinct taxa that are not often considered in the literature. These include angle of wing flexion/extension at joins in the distal forelimb, as well as tertiary lengths and propatagial dimensions, which are rarely able to be estimated in fossil taxa but greatly influence estimation of surface area (Tables 1 and S3).

Lithornithids provide key evidence of wing shape and flight style diversity in palaeognaths outside of the range observed in extant species in the clade (Houde, 1988; Nesbitt and Clarke, 2016). Reconstruction of ancestral characteristics in palaeognaths must account for not only the phylogenetic position of lithornithids but this diversity. Our results indicate that a capacity for sustained flight

was present in stem palaeognaths as recently as the late Paleocene. The ancestor of extant palaeognaths may also have been capable of sustained flight. That early divergences within Palaeognathae were possibly marked by flighted dispersal is consistent with recent phylogenomic and phylogeographic investigations of palaeognath evolution (Harshman et al., 2008; Mitchell et al., 2014; Yonezawa et al., 2017).

ACKNOWLEDGEMENTS

We thank C. Milensky (USNM) for specimen access and X. Wang (University of Jinan) for specimen photos. We thank D. Cannatella (U of Texas at Austin [UT]), N. Crouch (UT), S. Davis (UT), C. Eliason (UT), S. English (UT), D. Hillis (UT), S. Hood (UT), D. Ksepka (Bruce Museum), D. Lawver (Stony Book University) G. Musser (UT), S. Nesbitt (Virginia Tech), J. Proffitt (UT), and H. Zakon (UT) for comments and discussion. We also thank the editor, P. Dodson (University of Pennsylvania), and two anonymous reviewers for invaluable comments and recommendations. We are grateful for funding from the US National Science Foundation in support of this research (NSF EAR 1355292 to JAC).

LITERATURE CITED

Alerstam T, Rosén M, Bäckman J, Ericson PGP, Hellgren O. 2007. Flight speeds among bird species: Allometric and phylogenetic effects. PLoS Biol 5:e197.

Baker AJ, Haddrath O, McPherson JD, Cloutier A. 2014. Genomic support for a Moa–Tinamou Clade and adaptive morphological convergence in flightless ratites. Mol Biol Evol 31:1686–1696.

Blem CR. 1975. Geographic variation in wing-loading of the House Sparrow. Wilson Bull 87:543–549.

Bowlin MS. 2007. Sex, wingtip shape, and wing-loading predict arrival date at a stopover site in the Swainson's Thrush (*Catharus ustulatus*). Auk 124:1388–1396.

Bruderer B, Peter D, Boldt A, Liechti F. 2010. Wing-beat characteristics of birds recorded with tracking radar and cine camera. Ibis 152:272–291.

Burns JG, Ydenberg RC. 2002. The effects of wing loading and gender on the escape flights of least sandpipers (*Calidris minutilla*) and western sandpipers (*Calidris mauri*). Behav Ecol Sociobiol 52: 128–136.

Campbell KE, Tonni EP. 1983. Size and locomotion in teratorns (Aves: Teratornithidae). Auk 100:390–403.

Clarke JA. 2004. Morphology, phylogenetic taxonomy, and systematics of Ichthyrnis and Apatornis (Avialae: Ornithurae). Bull Am Mus Nat Hist 286:1–179.

Davies SJJF. 2002. *Ratites and tinamous: Tinamidae, Rheidae, Dromaiidae, Casuariidae, Apterygidae, Struthionidae*. Oxford; New York: Oxford University Press. p 310.

Dial KP, Randall RJ, Dial TR. 2006. What use is half a wing in the ecology and evolution of birds? Bioscience 56:437–445.

Dunning JB, editor. 2008. *CRC handbook of Avian body masses*. Boca Raton: CRC Press. p 655.

Field DJ, Lynner C, Brown C, Darroch SAF. 2013. Skeletal correlates for body mass estimation in modern and fossil flying birds. PLoS One 8:e82000.

Gadow H. 1888. Remarks on the numbers and on the phylogenetic development of the remiges of birds. Proc Zool Soc Lond 56:655–686.

Harshman J, Braun EL, Braun MJ, Huddleston CJ, Bowie RCK, Chojnowski JL, Hackett SJ, Han K-L, Kimball RT, Marks BD, et al. 2008. Phylogenomic evidence for multiple losses of flight in ratite birds. Proc Natl Acad Sci USA 105:13462–13467.

Houde P. 1988. *Paleognathous birds from the early tertiary of the northern hemisphere*. Cambridge, Massachusetts: Nuttall Ornithological Club. p 148.

Houde P, Olson SL. 1981. Paleognathous carinate birds from the Early Tertiary of North America. Science 214:1236–1237.

KleinHeerenbrink M. 2017. Afpt: Tools for modelling of animal flight performance. R package version 1.0.0.

Ksepka DT. 2014. Flight performance of the largest volant bird. Proc Natl Acad Sci USA 111:10624–10629.

Livezey BC. 1989. Flightlessness in Grebes (Aves, podicipedidae): Its Independent Evolution in Three Genera. Evolution 43:29–54.

Livezey BC, Humphrey PS. 1986. Flightlessness in Steamer-Ducks (Anatidae: tachyeres): Its morphological bases and probable evolution. Evolution 40:540–558.

Lucas AM, Stettenheim PR. 1972. *Avain anatomy integument*. Washington, DC: Agricultural Research Service.

Mitchell KJ, Llamas B, Soubrier J, Rawlence NJ, Worthy TH, Wood J, Lee MSY, Cooper A. 2014. Ancient DNA reveals elephant birds and kiwi are sister taxa and clarifies ratite bird evolution. Science 344:898–900.

Navarro J, González-Solís J, Viscor G, Chastel O. 2008. Ecophysiological response to an experimental increase of wing loading in a pelagic seabird. J Exp Mar Biol Ecol 358:14–19.

Nesbitt SJ, Clarke JA. 2016. The anatomy and taxonomy of the exquisitely preserved Green River formation (Early Eocene) Lithornithids (Aves) and the relationships of Lithornithidae. Bull Am Mus Nat Hist 406:1–91.

Nudds RL, Rayner JMV. 2006. Scaling of body frontal area and body width in birds. J Morphol 267:341–346.

Parris DC, Hope S. 2002. New interpretations of birds from the Navesink and Hornerstown Formations, New Jersey, USA (Aves: Neornithes). In: Zhou Z, Zhang F, editors. *Proceedings of the 5th Symposium of the Society of Avian Paleontology and Evolution*. Beijing: Science Press. p 113–124.

Pennycuick CJ. 1975. Mechanics of flight. In: Farner DS, King JR, editors. *Avian biology*. London, England: Academic Press. p 1–75.

Pennycuick CJ. 1989. *Bird flight performance: A practical calculation manual*. New York: Oxford University Press. p 153.

Pennycuick CJ. 2008. *Modelling the flying bird*. Canada: Academic Press. p 480.

Phillips MJ, Gibb GC, Crimp EA, Penny D. 2010. Tinamous and Moa Flock together: Mitochondrial genome sequence analysis reveals independent losses of flight among ratites. Syst Biol 59:90–107.

R Core Team. 2018. *R: A language and environment for statistical computing*. Vienna: R Foundation for Statistical Computing.

Savile OBO. 1957. Adaptive evolution in the avian wing. Evolution 11:212–224.

Thomas ALR, Hedenstrom A. 1998. The optimum flight speeds of flying animals. J Avian Biol 29:469.

Van Tyne J, Berger AJ. 1976. *Fundamentals of ornithology*. New York: Wiley. p 808.

Venables WN, Ripley BD, Venables WN. 2002. *Modern Applied Statistics with S*. New York: Springer. p 495.

Vickers-Rich P, Scarlett RJ. 1977. Another look at Megaegotheles, a large Owlet-Nightjar from New Zealand. Emu - Austral Ornithol 77:1–8.

Witter MS, Cuthill IC. 1993. The ecological costs of avian fat storage. Philos Trans Biol Sci 340:73.

Yonezawa T, Segawa T, Mori H, Campos PF, Hongoh Y, Endo H, Akiyoshi A, Kohno N, Nishida S, Wu J, et al. 2017. Phylogenomics and morphology of extinct paleognaths reveal the origin and evolution of the ratites. Curr Biol 27:68–77.